Optimal Contact Force Distribution for Compliant Humanoid Robots in Whole-Body Loco-Manipulation Tasks

Edoardo Farnioli[1,2], Marco Gabiccini[1,2,3], Antonio Bicchi[1,2]

Abstract— The term *whole-body loco-manipulation* refers to the case in which a humanoid robot exploits contacts with the environment, both with the end-effectors and with its internal limbs, in order to balance, move and/or manipulate the environment. In such a situation, high degree of redundancy may not be sufficient to completely control the robot movements and/or the forces applied on the environment. This problem is tackled in this work by means of quasi-static analysis tools. The reduction of mobility and manipulability is studied introducing the *Fundamental Loco-Manipulation Matrix* (FLMM) and its *canonical form* (cFLMM). Relevant information on the system can be extracted from those, obtaining, e.g., the space of the *controllable contact forces*, and the *controllable displacements of the center of mass*. Furthermore, the best contact force distribution able to meet the friction cone constraints is demonstrated to be the solution of a convex optimization problem.

The validity of the proposed methods is verified in two numerical examples, where internal contacts affects the controllability of both forces and displacements. Numerical results show that is crucial to consider the correlations between contact forces in order to exert target actions on the environment while coping with friction limits on the whole set of contacts.

I. INTRODUCTION

Humanoid robotics is currently one of the most attractive fields in robotics research. Evidence of this is the growing number of humanoid robots developed by different research teams. Noticeable are the exemplars presented in [1], [2], [3], to mention just a few of them.

The great capabilities of such systems have the side effect of a considerable complexity in finding an optimal control strategy for the whole system. As explained in [4], only recently researchers started to face the problem of locomotion and manipulation as a whole (*loco-manipulation*), considering and taking advantage from the reciprocal influence that the two tasks have one on the other.

In [5] and [6], the authors address the problem of modeling and control humanoid robots in loco-manipulation tasks. In these works they propose an approach in which the different tasks (e.g. controlling the posture of the hands, controlling the position of the center of mass, etc...) are sorted according to pre-defined priorities. Consequently, taking advantage from the high-degree of redundancy, the authors use a hierarchical control structure, bringing the robot to efficiently accomplish the tasks assigned. Similar problems are considered also in [7], [8], [9], [10]. Relevant

[1]*Research Center "E. Piaggio", Università di Pisa, Largo Lucio Lazzarino 1, 56122 Pisa, Italy.*

[2]Department of Advanced Robotics, Istituto Italiano di Tecnologia, Via Morego 30, 16163 Genova, Italy.

[3]Department of Civil and Industrial Engineering, Università di Pisa, Largo Lucio Lazzarino 1, 56122 Pisa, Italy.
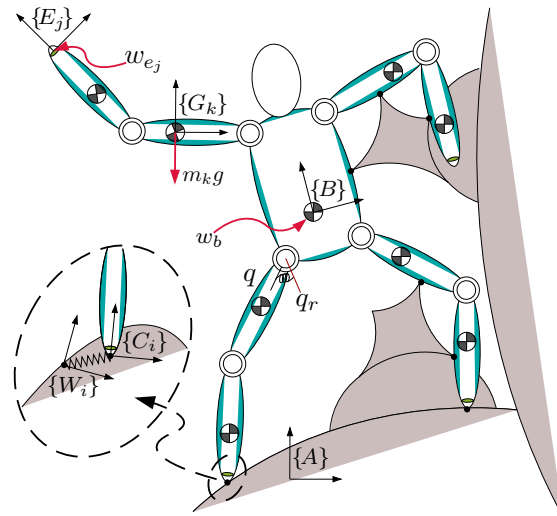
Fig. 1. Reference scenario for the description and the analysis of *whole-body loco-manipulation* tasks with humanoid robots.

is the contribution of [11], where the authors propose a new balancing control, based on the optimization of contact forces.

However, the methods discussed in those and in similar papers, are suited for contacts that occur on the extremal links of the robots or, more in general, under the assumption of a *full controllability* of the contact forces.

In some cases, however, the interaction with the environment is such to reduce the control capabilities of the robot. As an example, let us consider the situation sketched in Fig. 1. In such an unstructured scenario, the possibility to hang on the environment with the arms and/or the body certainly improves, or even allows to reach, the stability of the system. Considering the name proposed in [12] for equivalent conditions in manipulation tasks, we refer to these as *whole-body loco-manipulation* problems. In these cases, partial kinematic chains can become locally defective, jeopardizing both the mobility of the system and the controllability of the interaction forces.

To properly analyze these situations, we considered the analytical tools developed for grasping problems, where both the floating base (the grasped object) and the reduced controllability of contact forces (e.g. in case of whole-hand grasps) are managed concurrently, see for instance [13] and [14]. More recently, in [15] and [16], the derivative terms of the Jacobian matrix were introduced, in order to properly consider the influence of the contact force preload in the hand/object interaction.

In this paper, a general framework for the quasi-static analysis of *whole-body loco-manipulation* problems is presented. After the description of the system, in Sec. II, a method to point out some relevant properties of the system

is presented in Sec. III. By the definition of the *Fundamental Loco-Manipulation Matrix* (FLMM) and its *canonical form* (cFLMM), the subspace of the *controllable internal forces*, as well as the *controllable displacements of the reference link* and the *controllable displacements of the center of mass* are systematically found. Controllable internal forces are used in Sec. IV to formulate the contact force optimization problem, and to prove its convexity. The proposed approach selects *only* contact forces that the robot can actually apply on the environment, while keeping them the farthest possible from the friction cone edges (to guarantee a stability margin). Finally, in Sec. V, numerical examples are presented, showing how the proposed approach can be used to optimize the interaction force in whole-body loco-manipulation tasks.

II. SYSTEM MODELING

A. Reference Frames

With reference to Fig. 1, we introduce an inertial frame $\{A\}$ attached to the world, and a frame $\{B\}$ attached to the *reference link* of the robot, usually the torso or the waist. We will also refer to $\{B\}$ as the *floating base* of the robot.

For the ith contact point we introduce the frames $\{C_i\}$ and $\{W_i\}$, attached to the robot and to the world, respectively. Between them, a generalized virtual spring will describe the contact forces arising, as better explained in II-D.

For the jth end-effector not in contact with the environment, we consider a reference frame $\{E_j\}$ fixed with the robot. The origin of the frame $\{G_k\}$ coincides with the center of mass (CoM) of the kth link. During the motion of the robot, this frame remains always parallel to $\{A\}$, so that the gravity wrench of the kth CoM is constant in that frame.

These and other details about the notation are summarized in Table I.

B. Congruence Equations

In this section, we will provide a description of the displacements of the frames moving with the robot, that is $\{C_i\}, \{E_j\}$ and $\{G_k\}$. This will be a fundamental step to achieve both the description of the equilibrium of the system, by virtue of the kineto-static duality, and the characterization of the contact force variation as a function of the robot displacement (Sec. II-D).

First, we describe the motion of the frame $\{B\}$, attached to the reference link, with respect to the fixed frame $\{A\}$. To this aim, we introduce a *virtual kinematic chain* (VKC). For every configuration, the VKC should describe the configuration of $\{B\}$ with respect to $\{A\}$. For this reason, a convenient choice is to consider a kinematic chain composed by three prismatic joints, followed by three revolute joints.

Introducing $u \in \mathbb{R}^6$ as the vector of the joint parameter of the VKC, the spatial velocity of the floating base can be written as $\xi_{ab}^a = {}^aJ_{ab}(u)\dot{u}$, where ${}^aJ_{ab}(u) \in \mathbb{R}^{6 \times 6}$ is the *spatial Jacobian*[1] of the VKC.

Then, denoting with $\{P_r\}$, the rth frame moving with the robot, that is one among $\{C_i\}, \{E_j\}$ and $\{G_k\}$, its twist can be obtained as

$$\xi_{ap_r}^a = {}^aJ_{ap_r}(q^\star)\dot{q}^\star = \begin{bmatrix} {}^aJ_{ab}(u) & {}^aJ_{bp_r}(q) \end{bmatrix} \dot{q}^\star, \quad (1)$$

[1]For the details about the definition of *spatial* and *body* Jacobian matrices, as well as for the *adjoint transformation*, the reader can refer to [17].

Notation	Definition
δx	variation of variable x
$\bar{x}$	value of x in the equilibrium configuration
$\sharp x$	dimensions of vector x
$u \in \mathbb{R}^6$	joint parameters of the virtual kinematic chain, describing the configuration of $\{B\}$ with respect to $\{A\}$
$q \in \mathbb{R}^{\sharp q}$	joint parameters of the humanoid robot
$q^\star \in \mathbb{R}^{(6+\sharp q)}$	vector collecting virtual and real joint parameters as $q^\star := \begin{bmatrix} u^T & q^T \end{bmatrix}^T$
$\tau \in \mathbb{R}^{\sharp q}$	joint torques of the humanoid robot
$w_b \in \mathbb{R}^6$	external wrench acting on the reference link, parametrized as torques at the virtual kin. chain
$f_c \in \mathbb{R}^\kappa$	vector of contact forces/torques exerted by the robot on the world
$w_e \in \mathbb{R}^\epsilon$	vector of external wrenches acting on the free frames of the robot
$\xi_{xy}^z \in \mathbb{R}^6$	twist of frame $\{Y\}$ with respect to $\{X\}$, in components $\{Z\}$
${}^zJ_{xy} \in \mathbb{R}^6$	Jacobian of the kinematic chain describing the motion of $\{Y\}$ with respect to $\{X\}$, in components $\{Z\}$
${}^pS \in \mathbb{R}^{6 \times r}$	*humanoid stance* matrix in distal frames
${}^pJ \in \mathbb{R}^{r \times 6}$	humanoid Jacobian matrix in distal frames
$\Phi^\star$	*Fundamental Loco-Manipulation Matrix* (FLMM)
Φ	*Fundamental Loco-Manipulation Matrix* in canonical form (cFLMM)
φ	*augmented configuration*, vector collecting all the kineto-static variables of the system

TABLE I

NOTATION FOR WHOLE-BODY LOCO-MANIPULATION ANALYSIS.

where $q \in \mathbb{R}^{\sharp q}$ is the vector of the joint parameters of the real robot, $q^\star := \begin{bmatrix} u^T & q^T \end{bmatrix}^T \in \mathbb{R}^{6+\sharp q}$ is a vector collecting virtual and real joint parameters, and ${}^aJ_{bp_r}(q) \in \mathbb{R}^{6 \times \sharp q}$ is the Jacobian matrix describing the relative motion of $\{P_r\}$ with respect to $\{B\}$, with components in $\{A\}$.

Considering the adjoint[1] matrix $\text{Ad}_{g_{p_r a}}$, the frame twist in *body* components can be expressed as $\xi_{ap_r}^{p_r} = \text{Ad}_{g_{p_r a}(q^\star)} \xi_{ap_r}^a$. Applying this to (1), the twist of $\{P_r\}$ can be also written as

$$\xi_{ap_r}^{p_r} = {}^{p_r}J_{ap_r}(q^\star)\dot{q}^\star = \begin{bmatrix} {}^{p_r}J_{ab}(q^\star) & {}^{p_r}J_{bp_r}(q^\star) \end{bmatrix} \dot{q}^\star. \quad (2)$$

With $B_r^T \in \mathbb{R}^{\pi_r \times 6}$ we denote a selection matrix able to extract the components in interest from a given twist vector. In particular, for frames of the type $\{C_i\}$, corresponding to contacts with the environment, the selection matrix extracts only those components of the twist violating the contact constraint. As we will discuss in Sec. II-D, the contact constraint will be relaxed, by introducing a virtual spring. Motion directions selected by B_r^T will be those along which the interaction forces can be generated. The dimension π_r depends on the nature of the contact considered. As an example we report the case of the *hard finger* contact type, where only the three components of linear velocity are maintained, thus $\pi_r = 3$. For a detailed discussion of the contact types and on the selection matrices B_r^T, the reader can refer to [17].

For robot frames of type $\{E_j\}$, corresponding to end-effectors without contacts, no selection is needed in general. Finally, for frames of the type $\{G_k\}$, only the three terms corresponding to the linear velocity has to be kept, so $\pi_r = 3$.

Applying the selection matrix to (2), we can write

$$v_{ap_r}^{p_r} := B_r^T \xi_{ap_r}^{p_r} = \begin{bmatrix} B_r^T {}^{p_r}J_{ab}(q^\star) & B_r^T {}^{p_r}J_{bp_r}(q^\star) \end{bmatrix} \dot{q}^\star, \quad (3)$$

where $v_{ap_r}^{p_r} \in \mathbb{R}^{\pi_r}$ is the vector of the selected components of the twist. From Eq. (3) we can obtain the displacement of the frame $\{P_r\}$, indicated as δP_r, by multiplying each member for dt, obtaining

$$\delta P_{ap_r}^{p_r} = \begin{bmatrix} B_r^{T\,p_r} J_{ab}(q^\star) & B_r^{T\,p_r} J_{bp_r}(q^\star) \end{bmatrix} \delta q^\star. \quad (4)$$

Considering a total number of t robot frames, we group together all the frame displacements in the variable $\delta P_{ap}^p := \begin{bmatrix} \delta P_{ap_1}^{p_1^T}, \ldots, \delta P_{ap_t}^{p_t^T} \end{bmatrix}^T \in \mathbb{R}^\pi$, where $\pi := \sum_{r=1}^t \pi_r$.

In continuity with [10], let us define the *humanoid stance matrix in distal frame* as $^pS := \begin{bmatrix} B_1^{T\,p_1} J_{ab} & \ldots & B_t^{T\,p_t} J_{ab} \end{bmatrix} \in \mathbb{R}^{6 \times \pi}$. Similarly, let us define the Jacobian matrix of the humanoid robot in distal frames, as $^pJ := \begin{bmatrix} B_1^{T\,p_1} J_{bp_1} & \ldots & B_t^{T\,p_t} J_{bp_t} \end{bmatrix}^T \in \mathbb{R}^{\pi \times 6}$. With these definitions the displacements of all the robot frames can be written as

$$\delta P_{ap}^p = \begin{bmatrix} ^pS^T & ^pJ \end{bmatrix} \begin{bmatrix} \delta u \\ \delta q \end{bmatrix}, \quad (5)$$

where the dependency of the matrices on the system variables is omitted for the sake of compactness.

With a similar notation, considering the three types of robot frames in Fig. 1, we can write

$$\delta C_{ac}^c = \begin{bmatrix} ^cS^T & ^cJ \end{bmatrix} \begin{bmatrix} \delta u \\ \delta q \end{bmatrix}, \quad (6)$$

$$\delta E_{ae}^e = \begin{bmatrix} ^eS^T & ^eJ \end{bmatrix} \begin{bmatrix} \delta u \\ \delta q \end{bmatrix}, \quad (7)$$

$$\delta G_{ag}^g = \begin{bmatrix} ^gS^T & ^gJ \end{bmatrix} \begin{bmatrix} \delta u \\ \delta q \end{bmatrix}. \quad (8)$$

C. Displacement of the CoM

During the interaction with the environment it is often useful to know whether the action performed by the robot will influence the position of the CoM. To this aim, we call m_k the mass of the kth link of the robot, and $m = \sum_{k=1}^n m_k$ its total mass. By the definition of the CoM, considering the properties of the matrices $\{G_k\}$, and calling $\delta G \in \mathbb{R}^3$, the displacement of the CoM, it holds that

$$\delta G = \frac{1}{m} \sum_{k=1}^n m_k \delta G_{ag_k}^{g_k} \quad (9)$$

We note, in passing, that the displacements are formally referred to different frames of reference. It is anyway perfectly legal to add them up considering that, by definition, the terms involve only linear displacements, and that all the frames $\{G_k\}$ are parallel to $\{A\}$: thus all the contributions can be considered as expressed in the spatial frame.

From Eq. (9), it is straightforward to obtain the form

$$\delta G = \frac{1}{m} \begin{bmatrix} m_1 I_{g_1} \cdots m_n I_{g_n} \end{bmatrix} \begin{bmatrix} \delta G_{ag_1}^{g_1} \\ \vdots \\ \delta G_{ag_n}^{g_n} \end{bmatrix} := M \delta G_{ag}^g, \quad (10)$$

where the $I_{g_k} \in \mathbb{R}^{3 \times 3}$ are identity matrices. Finally, considering (8), the displacement of the CoM can be written as

$$\delta G = \begin{bmatrix} M^gS^T & M^gJ \end{bmatrix} \begin{bmatrix} \delta u \\ \delta q \end{bmatrix}. \quad (11)$$

D. Equilibrium of the System

The equilibrium equations of the system can be found by usual kineto-static duality arguments. From the displacements of the robot frames described in (5), introducing $\lambda \in \mathbb{R}^\pi$ collecting all the forces/moments acting on the robot frames, the equilibrium conditions for the humanoid robot can be properly written as

$$\begin{bmatrix} w_b \\ \tau \end{bmatrix} = \begin{bmatrix} ^pS \\ ^pJ^T \end{bmatrix} \lambda. \quad (12)$$

In (12) we denoted with $\tau \in \mathbb{R}^{\sharp q}$ the vector of the joint torques of the robot, and with $w_b \in \mathbb{R}^6$ a vector collecting the joint torques of the virtual kinematic chain. It is worth observing that, even if the vector w_b refers to *virtual* torques, it actually has an evident physical meaning. In fact, the vector w_b can be interpreted as a parametrization, in terms of joint torques, of an external wrench (disturbance) acting on the reference link of the robot.

As seen in (6), (7) and (8), matrices ^pS and $^pJ^T$ can be split in three parts, in order to highlight separately the displacements of the three types of robot frames. A similar operation can be done for the interaction vector by writing it as $\lambda = \begin{bmatrix} f_c^T & -w_e^T & -g^T \end{bmatrix}^T$, where the sign of the terms w_e and g is changed to represent forces actually exerted by the robot. Each part of the the vector λ is peculiar. In fact, the vector $f_c \in \mathbb{R}^\kappa$ collects all the force/moments that the humanoid exerts on the environment. To describe the interaction we consider a linear elastic penalty formulation. In this model the behavior of the ith contact force is synthesized by introducing a virtual spring acting between the frame $\{C_i\}$, attached to the robot, and the frame $\{W_i\}$, attached to the world[2]. In other words, considering the contact stiffness matrix $K_c \in \mathbb{R}^{\kappa \times \kappa}$, the contact force variation and the contact frame displacement are related by

$$\delta f_c = K_c \delta C_{wc}^c, \quad (13)$$

that defines the *constitutive equation of the contact*.

Taking into account (6), from (13) it follows that the contact force variation can be described as

$$\delta f_c = K_c \left(^cS^T \delta u + {}^cJ \delta q \right). \quad (14)$$

The vector $w_e \in \mathbb{R}^\epsilon$ collects all the external wrenches (disturbances) acting on the end-effectors of the robot that are not in contact with the environment. Finally, the vector $g \in \mathbb{R}^\gamma$ groups all the gravity forces acting on each CoM of the robot links. It is worth observing that, thanks to the properties of the frames $\{G_k\}$, this vector is constant for every configuration of the humanoid robot.

E. Quasi-Static Formulation of the Equilibrium Equations

In order to obtain a quasi-static description of the equilibrium laws of the system, we compute the first order approximation of (12). Considering the properties of each interaction vector, we obtain

$$\delta w_b = {}^c\bar{S}\delta f_c - {}^e\bar{S}\delta w_e + \bar{U}_s \delta u + \bar{Q}_s \delta q, \quad (15)$$

$$\delta \tau = {}^c\bar{J}^T \delta f_c - {}^e\bar{J}^T \delta w_e + \bar{U}_j \delta u + \bar{Q}_j \delta q, \quad (16)$$

[2]The reader can find more details about the elastic contact model in [16].

where $\bar{U}_s := \left.\frac{\partial^p S\lambda}{\partial u}\right|_0 \in \mathbb{R}^{6\times 6}$, $\bar{Q}_s := \left.\frac{\partial^p S\lambda}{\partial q}\right|_0 \in \mathbb{R}^{6\times \sharp q}$, $\bar{U}_j := \left.\frac{\partial^p J^T\lambda}{\partial u}\right|_0 \in \mathbb{R}^{\sharp q\times 6}$, $\bar{Q}_j := \left.\frac{\partial^p J^T\lambda}{\partial q}\right|_0 \in \mathbb{R}^{\sharp q\times \sharp q}$.

Eq. (15) describes the equilibrium of the floating base, taking into account the external wrenches, the contact force variation and the effects due by the variation of the robot configuration. Finally, Eq. (16) describes the equilibrium of the humanoid robots at the joint level, when similar perturbations occur.

F. Elastic Joint Model

The equations presented up to here can describe the quasi-static behavior of a rigid humanoid robot. However, today's robot need a certain amount of physical compliance, in order to safely interact with humans and/or to safely absorb impacts. This feature is often introduced by the designer as a physical rotational spring connecting the motor shaft and the rigid link. Indicating with $q_r \in \mathbb{R}^{\sharp q}$ the vector of the motor position, acting as a *reference* for the joint configuration q, and indicating with $K_q \in \mathbb{R}^{\sharp q \times \sharp q}$ a matrix collecting all the joint stiffness values, the quasi-static equation describing the equilibrium of the elastic joint can be written as

$$\delta\tau = K_q\left(\delta q_r - \delta q\right). \tag{17}$$

III. THE FUNDAMENTAL LOCO-MANIPULATION EQUATION

The set composed by the *congruence equation* in (5), of the *CoM displacement* in (11), the *constitutive equation of the contacts* in (13) and, finally, the *equilibrium equations*, both for the floating base in (15), and for the joints in (16) provide a complete description of the quasi-static behavior of the system. Considering that (5) was substituted already in (13), giving (14), by gathering all the eq.s in a system we obtain a compact equation called *Fundamental Loco-Manipulation Equation* (FLME), that appears in the form

$$\Phi^\star \delta\varphi = 0, \tag{18}$$

where

$$\Phi^\star = \begin{bmatrix} I_f & 0 & -K_c{}^c\bar{S}^T & 0 & -K_c{}^c\bar{J} & 0 & 0 & 0 \\ -{}^c\bar{J}^T & I_\tau & -\bar{U}_j & 0 & -\bar{Q}_j & 0 & {}^e\bar{J}^T & 0 \\ -{}^c\bar{S} & 0 & -\bar{U}_s & 0 & -\bar{Q}_s & I_{w_b} & {}^e\bar{S} & 0 \\ 0 & 0 & -M^g\bar{S}^T & I_g & -M^g\bar{J} & 0 & 0 & 0 \\ 0 & I_\tau & 0 & 0 & K_q & 0 & 0 & -K_q \end{bmatrix}, \tag{19}$$

$$\delta\varphi = \begin{bmatrix} \delta f_c^T & \delta\tau^T & \delta u^T & \delta G^T & \delta q^T & \delta w_b^T & \delta w_e^T & \delta q_r^T \end{bmatrix}^T. \tag{20}$$

The FLME in (18), clearly is a *linear* and *homogeneous* system of equations. The coefficient matrix of the system, in (19), $\Phi^\star \in \mathbb{R}^{r_\Phi \times c_\Phi}$, is also called the *Fundamental Loco-Manipulation Matrix* (FLMM), and $\delta\varphi \in \mathbb{R}^{\sharp\varphi}$, in (20), is the variation of the *augmented configuration* of the system. Considering the structure of the FLMM, it is easy to verify that its dimensions are such that

$$\begin{cases} r_\Phi = \kappa + 2\sharp q + 9 \\ c_\Phi = \kappa + 3\sharp q + \epsilon + 15. \end{cases} \tag{21}$$

It is possible to prove that the FLMM is always full-row rank[3], regardless of the particular system configuration. Considering this, from (21) it directly follows that the solution

[3]A proof regarding the rank of the FLMM is avoided here for space limitations.

space of (18) can be found in the basis of the nullspace of the FLMM, that is employing a matrix $\Gamma \in \mathbb{R}^{c_\Phi \times (c_\Phi - r_\Phi)}$, with $c_\Phi - r_\Phi = \sharp q + \epsilon + 6$, such that $\Phi^\star \Gamma = 0$.

A. Canonical Form of the FLMM

Defining the vector of the *independent variables* as

$$\delta\varphi_i = \begin{bmatrix} \delta w_b^T & \delta w_e^T & \delta q^T \end{bmatrix}^T \in \mathbb{R}^{c_\Phi - r_\Phi}, \tag{22}$$

and labeling the remaining part of the augmented configuration as the *dependent variables* $\delta\varphi_d \in \mathbb{R}^{r_\Phi}$, from (18) it follows that

$$\begin{bmatrix} \Phi_d^\star & \Phi_i^\star \end{bmatrix} \begin{bmatrix} \delta\varphi_d \\ \delta\varphi_i \end{bmatrix} = 0. \tag{23}$$

Apart from very few pathological situations, of limited interest, it results[4] that $\text{rank}(\Phi_d^\star) = c_\Phi$. Because of this, we can left-multiply (23) by $(\Phi_d^\star)^{-1}$, thus obtaining

$$\begin{bmatrix} I & \Phi_i \end{bmatrix} \begin{bmatrix} \delta\varphi_d \\ \delta\varphi_i \end{bmatrix} = 0, \tag{24}$$

where $\Phi_i := (\Phi_d^\star)^{-1}\Phi_i^\star$. Eq. (24) defines the *Canonical form of the Fundamental Loco-Manipulation Equation* (cFLME), and we call its coefficient matrix, characterized by the presence of an identity block, the *Canonical form of the Fundamental Loco-Manipulation Matrix* (cFLMM). More in detail, the cFLME can be written in the form

$$\begin{bmatrix} I_f & 0 & 0 & 0 & 0 & {}^bW_f & {}^eW_f & R_f \\ 0 & I_\tau & 0 & 0 & 0 & {}^bW_\tau & {}^eW_\tau & R_\tau \\ 0 & 0 & I_u & 0 & 0 & {}^bW_u & {}^eW_u & R_u \\ 0 & 0 & 0 & I_g & 0 & {}^bW_g & {}^eW_g & R_g \\ 0 & 0 & 0 & 0 & I_q & {}^bW_q & {}^eW_q & R_q \end{bmatrix} \begin{bmatrix} \delta f_c \\ \delta\tau \\ \delta u \\ \delta G \\ \delta q \\ \delta w_b \\ \delta w_e \\ \delta q_r \end{bmatrix} = 0. \tag{25}$$

From (24) it is evident that the *dependent* variables of the system can be computed as a function of the *independent* variables as $\delta\varphi_d = -\Phi_i\delta\varphi_i$.

B. Relevant Properties of the cFLMM

Some blocks composing the cFLMM provide interesting information on the system. For example, from the first equation, in (25), it follows that, when no external disturbance is present, all the contact forces that can be realized by robot are in the range space of the matrix R_f. Put differently, matrix R_f spans the *controllable internal forces*. Similarly, the range space of R_u represents the space of *controllable displacements of the reference link* (e.g. the torso) of the robot. It is also interesting to highlight that matrix R_g describes the movement of the CoM consequent to the robot joint displacements, thus parameterizing the *controllable displacement of the CoM*. Finally, when joint variables are held fixed ($\delta q_r = 0$), matrices ${}^bW_u$ and ${}^eW_u$ describe how an external wrench acting *on the reference link* and *on the free end-effectors*, respectively, affect the reference link configuration itself.

[4]The fact that the FLMM is full rank does not guarantee that the block $\Phi_d^\star$ is actually invertible. However, to the best of our knowledge and experience, we can assert that, if exceptions are analytically possible, they refer to pathological situations of poor practical relevance.

IV. Convexity of the Force Optimization Problem in Whole-Body Loco-Manipulation Tasks

In every working condition, from simple stance tasks, to whole-body interactions, the problem of properly managing contact forces is a relevant one. If robot-environment interactions are to be used to improve the stability of the robot or to prevent slippage, accurate modeling of the actual force components that the robot can exert on the environment becomes crucial. To this sake, besides a description of the controllable forces, friction cone constraints have also to be considered.

For the sake of simplicity, we will focus our analysis on the case of contact point with friction (aka *hard finger*). However, the generalization of the following considerations poses no difficulties.

In the following, we will indicate with f_{c_i} and n_i the contact force and the normal vector at the ith contact point. Moreover, the symbol $\mathcal{C}$ will indicate the set of all the contact points. With this notation, the friction cone constraint, can be expressed by Coulomb's inequality as

$$\sigma_{i,\text{frict}} = \alpha_i \|f_{c_i}\| - f_{c_i}^T n_i \leq 0, \qquad \forall\, i \in \mathcal{C}, \tag{26}$$

where[5] $\alpha_i \in \mathbb{R}^+$.

Similarly, denoting with $f_{\min_i}$ and $f_{\max_i}$ the value of the minimum and maximum force admitted on the ith contact point, the corresponding constraints can be expressed as

$$\sigma_{i,\min} = \quad f_{\min_i} - f_{c_i}^T n_i \leq 0, \tag{27}$$

$$\sigma_{i,\max} = -f_{\max_i} + f_{c_i}^T n_i \leq 0. \tag{28}$$

Defining $\mathcal{T}$ as the set of constraint types, such that $\mathcal{T} = \{\text{frict}, \min, \max\}$, the contact constraints seen in (26), (27) and (28) can be synthesized as

$$\sigma_{i,j} = \alpha_{i,j} \|f_{c_i}\| + \beta_{i,j} f_{c_i}^T n_i + \gamma_{i,j} \leq 0, \tag{29}$$

where $i \in \mathcal{C}$, $j \in \mathcal{T}$. In Table II, the values of the coefficients are summarized for the different cases.

	$\alpha_{i,j}$	$\beta_{i,j}$	$\gamma_{i,j}$
frict	$\alpha_i > 0$	-1	0
min	0	-1	$f_{\min_i}$
max	0	1	$-f_{\max_i}$

TABLE II
COEFFICIENT VALUES FOR CONTACT CONSTRAINTS IN (29).

For the ith contact point and for the jth contact constraint type, we introduce the function

$$V_{i,j} = \begin{cases} (2\sigma_{i,j})^{-1} & \text{if } \sigma_{i,j} < \varepsilon, \ \forall i \in \mathcal{C}, \ j \in \mathcal{T}, \\ a\sigma_{i,j}^2 + b\sigma_{i,j} + c & \text{otherwise.} \end{cases} \tag{30}$$

By imposing continuity conditions in ε, we can find $a = \frac{3}{2\varepsilon^4}$, $b = \frac{4}{\varepsilon^3}$, $c = \frac{3}{\varepsilon^2}$.

With the previous definitions, the function

$$V = \sum_{i \in \mathcal{C}} \sum_{j \in \mathcal{T}} V_{i,j} \tag{31}$$

can be associated to the system configuration. We can also say that Eq. (31) encodes global information about

[5]The coefficient α is related to the friction coefficient μ through the relation $\alpha_i = 1/\sqrt{1 + \mu_i^2}$.

the distance of the system from the contact limits. More precisely, lower values of V_{ij} correspond to greater distance to the contact margins, if the bound limits imposed by (26), (27) and (28) are complied. Consequently, a minimum of V in (31) correspond to the optimal contact force distribution in terms of distance from the contact limits, along the metrics defined by (30).

In order to investigate the properties of (31), we compute its derivatives. For later use, let us introduce matrix $E \in \mathbb{R}^{\kappa \times \rho_f}$ representing a basis for the span of R_f in (18), and ρ_f is its rank. With this notation every contact force variation can be written as $\delta f_c = Ey$, where $y \in \mathbb{R}^{\rho_f}$ is a coefficient vector. Similarly, the ith contact force variation can be written as $\delta f_{c_i} = E_i y$, where $E_i \in \mathbb{R}^{\kappa_i \times \rho_f}$ is a proper portion of the basis E.

It is not difficult to find out that the Hessian matrix of (31) can be written as summation of terms in the form

$$\frac{\partial^2 \sigma_{i,j}}{\partial y^2} = \frac{\alpha_{i,j}}{\|f_{c_i}\|} E_i^T \left(I - \frac{f_{c_i}^T f_{c_i}}{\|f_{c_i}\|^2} \right) E_i, \tag{32}$$

$$\frac{\partial \sigma_{i,j}}{\partial y} \frac{\partial \sigma_{i,j}}{\partial y}^T = \frac{\alpha_{i,j}^2}{\|f_{c_i}\|^2} f_{c_i} f_{c_i}^T. \tag{33}$$

Eq.s (32) and (33) clearly represent symmetric positive semidefinite matrices. This implies that the Hessian is, at least, a positive semidefinite matrix as well. Moreover, the Hessian matrix can be positive definite if the two terms do not vanish at the same time. In other words, we have to verify if a vector x exists such that

$$\begin{cases} x^T \left(\dfrac{\partial^2 \sigma_{i,j}}{\partial y^2} \right) x = 0 \\ x^T \left(\dfrac{\partial \sigma_{i,j}}{\partial y} \dfrac{\partial \sigma_{i,j}}{\partial y}^T \right) x = 0. \end{cases} \tag{34}$$

For the ith contact point, it is easy to find that the first condition of the system in (34), evaluated for the friction constraint implies that (i) $E_i x$ is parallel to n_i. On the contrary, considering the constraints on minimum and maximum force, from the second condition in (34) it follows that (ii) $n_i^T E_i x = 0$. Clearly, the two previous conditions can be verified at the same time iff $E_i x = 0$. Considering that this result has to hold for every contact, by juxtaposing all the relationships we obtain the condition $Ex = 0$. Remembering that matrix E was defined as a *basis* for the controllable internal forces, it follows that

$$x^T \frac{\partial^2 V}{\partial y^2} x > 0 \qquad \forall x \neq 0, \tag{35}$$

that finally proves that function V in (31) is strictly convex.

Moreover, direct application of the definition is enough to verify that the constraints (26), (27) and (28) form a convex set. Summing up, finding the minimum of the function (31), subject to the constraints (26), (27) and (28) reduces to solve a *convex optimization problem*.

Once the optimal contact force variation δf_c^{opt} is found, considering the first equation of the system (25), a straightforward computation of the relative joint reference variation follows in the form

$$\delta q_r^{\text{opt}} = -R_f^\dagger \delta f_c^{\text{opt}}, \tag{36}$$

if no external disturbance acts on the robot. Moreover, generally speaking, the matrix R_f is not a basis. Thus,
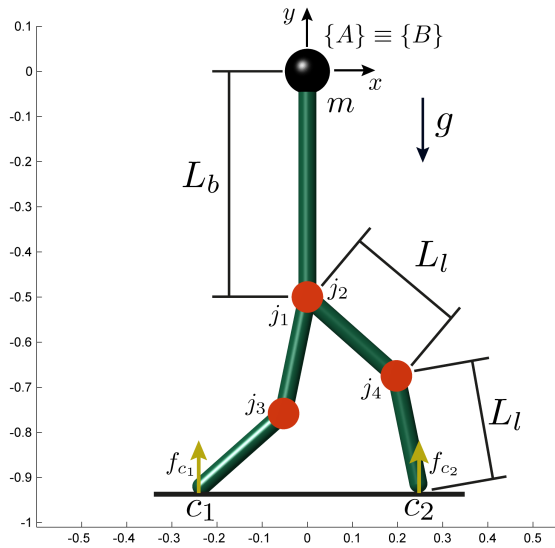
Fig. 2. A humanoid robot upright in a vertical plane. The robot is touching the floor with the feet, on a plane with variable inclination and friction.

considering a matrix Γ_{R_f} such that $R_f \Gamma_{R_f} = 0$, all the possible joint reference variation corresponding to δf_c^{opt} can be written as $\delta q_r^{\text{opt}} = -R_f^\dagger \delta f_c^{\text{opt}} + \Gamma_{R_f} z$, where z is a suitable coefficient vector.

V. NUMERICAL EXAMPLES

A. Humanoid Robot Approaching a Slope

As a first example, we consider a humanoid robot standing upright, approaching a slope. With reference to Fig. 2 and 3, in all the cases, the left contact in c_1 is touching a horizontal surface. The inclination angle θ and the friction coefficients μ_1 and μ_2 take on different values, depending on the case studied.

In the initial configuration, the fixed frame $\{A\}$ and the floating frame $\{B\}$ coincide. Their origin is placed on the initial position of the CoM of the robot (black sphere in Fig. 2). The gravity force applied to the CoM is $mg = -500$ N. A virtual kinematic chain (not represented) composed by two prismatic joints, with axis aligned with x and y respectively, and one revolute joint, with axis aligned with z, connects them. The torso of the robot is sketched with a link of length $L_b = 0.5$ m, and it is the only heavy element in the analysis, consequently the CoM is attached to it. Two revolute joints j_1 and j_2 can independently move the legs with respect to the torso. The revolute joints j_3 and j_4 serve as knees. Each link of the legs has length $L_l = L_b/2$. In all the examples, in the initial configuration the torso is aligned with the y axis. Moreover, the joint configuration is such that the triangle c_1–j_1–c_2 is equilateral, with side of length L_b. The initial contact forces at the contacts are vertical with module such to ensure the equilibrium. All the contacts are *hard finger*. The contact stiffness and the joint stiffness values are set to $k_c = 10^8$ N/m and $k_q = 10^4$ Nm/rad for all the contacts and the joints, respectively.

In this example, the optimization approach described above, is used to balance the humanoid, taking into account the direction of the normal vector and the friction coefficient at the contacts. It is interesting to note that, even if the contact force vector has dimension four, and the robot is equipped

with four actuated joints, in this case, the controllable contact forces are spanned by $E \in \mathbb{R}^{4 \times 2}$.

Let us discuss more in detail the case in which the inclination of the slope is $\theta = 20°$, and we impose the limits $f_{\min} = 0$ N and $f_{\max} = 500$ N, for all the contacts.

The initial contact forces are

$$f_{c_1} = \begin{bmatrix} 0 & 407.6 \end{bmatrix}^T, \quad f_{c_2} = \begin{bmatrix} 0 & 92.4 \end{bmatrix}^T. \quad (37)$$

When $\mu_1 = \mu_2 = 1$, the optimization method, considering the controllability of the contact forces, provides the result sketched in Fig. 3(b). The optimized contact force values (exerted by the environment on the robot) are

$$f_{c_1} = \begin{bmatrix} 66.4 & 268.8 \end{bmatrix}^T, \quad f_{c_2} = \begin{bmatrix} -66.4 & 231.2 \end{bmatrix}^T. \quad (38)$$

Once the optimal contact force variation is found, the minimal joint reference perturbation able to apply it is obtained via (36). Finally, the corresponding joint perturbation is found considering that from (25) it follows $\delta q = -R_q \delta q_r$, in case of no external disturbances. The case represented in 3(b) corresponds to the joint displacements $\delta q = \begin{bmatrix} 0.17 & 0.29 & 0.11 & -0.12 \end{bmatrix}^T$. Similarly, when $\mu_1 = 1$ and $\mu_2 = 0.5$ (Fig. 3(c)), the optimization suggests to move the CoM forward, in order to better align the contact force on c_2, with the normal direction at the contact. The optimized contact forces result

$$f_{c_1} = \begin{bmatrix} 91.5 & 216.3 \end{bmatrix}^T, \quad f_{c_2} = \begin{bmatrix} -91.5 & 283.7 \end{bmatrix}^T, \quad (39)$$

corresponding to the joint displacements $\delta q = \begin{bmatrix} 0.24 & 0.40 & 0.15 & -0.17 \end{bmatrix}^T$.

In the case $\mu_1 = 0.1$ and $\mu_2 = 1$ (Fig. 3(e)), the optimization result proposes to move backward the CoM, encouraging the alignment of the contact force to the local normal at the point with less friction. Numerically, the final contact forces result

$$f_{c_1} = \begin{bmatrix} 2.6 & 466.0 \end{bmatrix}^T, \quad f_{c_2} = \begin{bmatrix} -2.6 & 34.0 \end{bmatrix}^T, \quad (40)$$

obtained for a joint configuration variation of $\delta q = \begin{bmatrix} -0.06 & -0.10 & -0.04 & 0.04 \end{bmatrix}^T$.

Similar behavior is shown also in the other tests, qualitatively presented in Fig. 3.

B. Pushing Humanoid Example

In the second example, sketched in Fig. 4, a humanoid robot is pushing a heavy object (fixed in the analysis). The humanoid is in contact with the ground with its feet, and with the object to be moved, by a knee, the torso and both the proximal and the distal links of the arm. Preload contact forces are considered at points c_1, c_2 and c_6. The torso is considered the only heavy element in the analysis.

In such a configuration, it appears clearly how the mobility and the capabilities of the robot are greatly reduced. In fact, the dimension of the controllable internal forces result $E \in \mathbb{R}^{12 \times 6}$. The contact force optimization tools were used, in this case, to find the maximum pushing force allowed. This was made by building an optimization function V, considering only the $\sigma_{i,\text{frict}}$ and $\sigma_{i,\text{min}}$ for all the contacts on the knee, the torso and the arm. All the other $\sigma_{i,j}$'s were treated as constraints in the optimization problem. For all the contacts, the minimum force is set to zero. The maximum contact force is set to $f_{\max} = mg = 500$ N for

(a) $\theta = 10°$, $\mu_1 = 1$, $\mu_2 = 1$ (b) $\theta = 20°$, $\mu_1 = 1$, $\mu_2 = 1$ (c) $\theta = 20°$, $\mu_1 = 1$, $\mu_2 = 0.5$ (d) $\theta = 20°$, $\mu_1 = 0.5$, $\mu_2 = 1$ (e) $\theta = 20°$, $\mu_1 = 0.1$, $\mu_2 = 1$
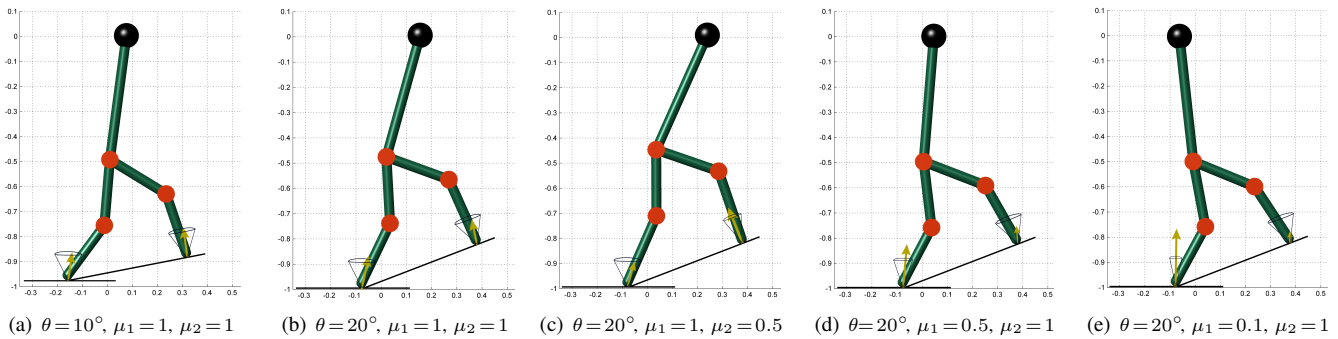
Fig. 3. In panel (a) is represented the optimized configuration of a humanoid robot approaching a surface with inclination $\theta = 10°$, with friction coefficients $\mu_1 = \mu_2 = 1$. Panels (b)−(e) show the result of the optimization for a surface with inclination $\theta = 20°$, varying the friction coefficients.

the legs, and $f_{\max} = mg/3$ N for the other contacts. Omitting a detailed discussion for space limitations, we report that in this condition the maximum pushing force possible that can meet the constraints results $f_x = 573.4$ N.

It is worth observing that, in such a whole-body loco-manipulation task, is crucial to properly consider the high coupling between the contact forces. This fact is distinctly shown by reformulating the problem removing the force limits at the feet. In this case, the maximum force limits are reached on the knee, the torso and the arm, resulting in a total pushing force of $f_x = 666.7$ N. To obtain this result, the contact forces needed on the feet are $f_{c_1} = [-705.1, 950.1]^T$ and $f_{c_2} = [426.0, -26.0]^T$, which would clearly violate the constraints in the previous case, thus showing the influence of the contact limits imposed to the feet on the maximum pushing force achievable.
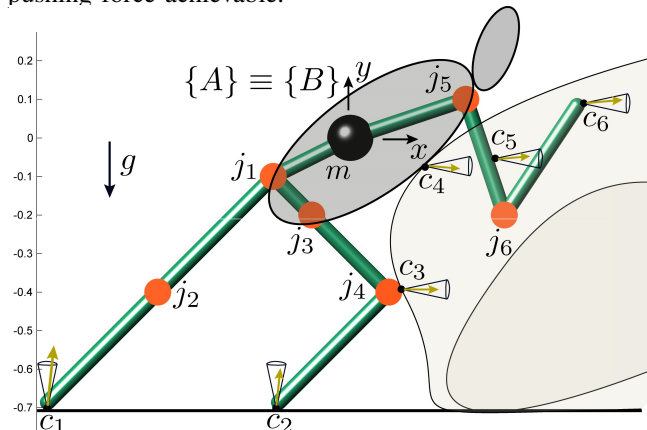
Fig. 4. A humanoid robot pushing a heavy object in a typical *whole-body loco-manipulation* task.

VI. CONCLUSIONS

In this paper, we presented a general framework for the analysis of humanoid robots in contact with the environment both with the end-effectors, and the internal links. We denote this aggregated problem with the term *whole-body loco-manipulation*. In such a situation, despite the high degree of redundancy, the capabilities of the robot can be greatly compromised.

After the discussion of the quasi-static equations of the system, a systematic way to find a basis for the *controllable internal forces*, together with other relevant properties of the system, is presented, based on the definition of the *fundamental loco-manipulation matrix*. Furthermore, for every contact, friction cone constraints, and minimum/maximum tolerable

forces were considered, also showing that the contact force optimization can be framed as a convex problem.

Finally, two numerical examples were shown, pointing out the importance of properly taking into account the mutual correlation between contact forces to met the contact limits.

REFERENCES

[1] K. Hirai, M. Hirose, Y. Haikawa, and T. Takenaka, "The development of honda humanoid robot," in *International Conference on Robotics and Automation (ICRA)*, pp. 1321–1326 vol.2, 1998.

[2] K. Kaneko, F. Kanehiro, M. Morisawa, K. Akachi, G. Miyamori, A. Hayashi, and N. Kanehira, "Humanoid robot hrp-4 - humanoid robotics platform with lightweight and slim body," in *International Conference on Intelligent Robots and Systems (IROS)*, 2011.

[3] N. Tsagarakis, S. Morfey, G. Cerda, L. Zhibin, and D. Caldwell, "Compliant humanoid coman: Optimal joint stiffness tuning for modal frequency control," in *International Conference on Robotics and Automation (ICRA)*, pp. 673–678, May 2013.

[4] O. Brock, D. Katz, and S. Srinivasa, "Mobile manipulation," in *IEEE Robotics and Automation Magazine*, pp. 18–19, 2012.

[5] L. Sentis and O. Khatib, "Synthesis of whole-body behaviors through hierarchical control of behavioral primitives.," *I. J. Humanoid Robotics*, vol. 2, no. 4, pp. 505–518, 2005.

[6] L. Sentis, J. Park, and O. Khatib, "Compliant control of multicontact and center-of-mass behaviors in humanoid robots.," *IEEE Transactions on Robotics*, vol. 26, no. 3, pp. 483–501, 2010.

[7] H. Arisumi, J.-R. Chardonnet, and K. Yokoi, "Whole-body motion of a humanoid robot for passing through a door - opening a door by impulsive force -.," in *IROS*, pp. 428–434, IEEE, 2009.

[8] O. Stasse, P. Evrard, N. Perrin, N. Mansard, and A. Kheddar, "Fast foot prints re-planning and motion generation during walking in physical human-humanoid interaction.," in *Humanoids*, pp. 284–289, 2009.

[9] A. Johnson and D. Koditschek, "Legged self-manipulation," *IEEE Access*, vol. 1, pp. 310–334, 2013.

[10] K. Shankar and J. W. Burdick, "Kinematics and methods for com-bined quasi-static stance/reach planning in multi-limbed robots," in *International Conference on Robotics and Automation, ICRA 2014.*

[11] C. Ott, M. Roa, and G. Hirzinger, "Posture and balance control for biped robots based on contact force optimization," in *International Conference on Humanoid Robots*, pp. 26–33, Oct 2011.

[12] K. Salisbury, "Whole arm manipulation," in *International Symposium on Robotics Research*, pp. 183–189, 1988.

[13] A. Bicchi, "On the problem of decomposing grasp and manipulation forces in multiple whole-limb manipulation," *Int. Journal of Robotics and Autonomous Systems*, vol. 13, pp. 127–147, 1994.

[14] A. Bicchi and D. Prattichizzo, "Manipulability of cooperating robots with unactuated joints and closed-chain mechanisms," *IEEE Trans. Robotics and Automation*, vol. 16, pp. 336–345, August 2000.

[15] M. Gabiccini, E. Farnioli, and A. Bicchi, "Grasp and manipulation analysis for synergistic underactuated hands under general loading conditions," in *International Conference of Robotics and Automation (ICRA)*, pp. 2836 – 2842, 2012.

[16] M. Gabiccini, E. Farnioli, and A. Bicchi, "Grasp analysis tools for synergistic underactuated robotic hands," *International Journal of Robotic Reasearch*, vol. 32, pp. 1553 – 1576, 11/2013 2013.

[17] R. Murray, Z. Li, and S. Sastry, *A mathematical introduction to robotic manipulation*. CRC Press, 1994.